

Journal of Materials Chemistry C

Accepted Manuscript



This is an *Accepted Manuscript*, which has been through the Royal Society of Chemistry peer review process and has been accepted for publication.

Accepted Manuscripts are published online shortly after acceptance, before technical editing, formatting and proof reading. Using this free service, authors can make their results available to the community, in citable form, before we publish the edited article. We will replace this *Accepted Manuscript* with the edited and formatted *Advance Article* as soon as it is available.

You can find more information about *Accepted Manuscripts* in the [Information for Authors](#).

Please note that technical editing may introduce minor changes to the text and/or graphics, which may alter content. The journal's standard [Terms & Conditions](#) and the [Ethical guidelines](#) still apply. In no event shall the Royal Society of Chemistry be held responsible for any errors or omissions in this *Accepted Manuscript* or any consequences arising from the use of any information it contains.

Wet-process feasible novel carbazole-type molecular host for high efficiency phosphorescent organic light emitting diodes

Jwo-Huei Jou^{a*}, Sudhir Kumar^a, Daiva Tavgeniene^b, Chih-Chia An^a, Po-Hsun Fang^a, Ernestas Zaleckas^b, Juozas V. Grazulevicius^b, Saulius Grigalevicius^{b*}

^aDepartment of Materials Science and Engineering, National Tsing-Hua University, Hsin-Chu-30013, Taiwan, ROC

^bDepartment of Polymer Chemistry and Technology, Kaunas University of Technology, Radvilenu plentas 19, LT50254, Kaunas, Lithuania

*Corresponding authors: jjou@mx.nthu.edu.tw (J.-H. Jou) and saulius.grigalevicius@ktu.lt (S. Grigalevicius)

Abstract

Wet-process organic light-emitting diodes (OLEDs) are crucial to realize cost-effective and large-area roll-to-roll fabrication of high quality displays and lightings. In this study, a wet-process feasible carbazole based host material, 2-[4-(carbazol-9-yl)butyloxy]-9-[4-(carbazol-9-yl)butyl]carbazole (**6**), is synthesized, and two other carbazole hosts, 2-[5-(carbazol-9-yl)penyloxy]-9-[5-(carbazol-9-yl)penyl]carbazole (**7**) and 2-[6-(carbazol-9-yl)hexyloxy]-9-[6-(carbazol-9-yl)hexyl]carbazole (**8**) are also synthesized for comparison. All three host materials exhibit high triplet energy, and possess high solubility in common organic solvents at room temperature. Doping a green phosphorescent emitter *fac* tris(2-phenylpyridine)iridium (Ir(ppy)₃) into host **6**, the device shows an efficacy of 51 lmW⁻¹ and current efficiency of 52 cdA⁻¹ at 100 cdm⁻² or 30 lmW⁻¹ and 40.7 cdA⁻¹ at 1,000 cdm⁻². The high efficiency may be attributed to the host possessing an effective host-to-guest energy transfer, the ability for excitons to generate on both host and guest, and excellent film integrity.

1. Introduction

Organic light emitting diode (OLED) is a potential technology to realize high quality displays and solid state lightings.¹⁻³ Nowadays, a wide range of OLED based portable display products and some large size displays have already been in the market.^{4,5} Recently, phosphorescent OLEDs have drawn great attention because of their ability to harvest both singlet and triplet excitons simultaneously through intersystem crossing, approaching near-100% internal

quantum efficiency.⁶⁻⁹ An appropriate molecular host material is required to minimize the concentration quenching effects and triplet-triplet annihilation in an undoped phosphorescent emitter¹⁰ A high-triplet energy molecular host material is crucial because it can be used to confine triplet excitons on the emitter and balance the carrier injection.¹¹⁻¹⁴

OLED devices can be fabricated by thermal evaporation and spin-coating deposition of organic molecular materials. Thermal evaporation seems to be a successful approach to achieve high efficiency with small molecular hosts. However, it is limited to numerous issues such as condition of high thermally stable organic molecules, low throughput and comparatively higher cost due to huge wastage of organic materials in the chamber itself. To make the resultant products highly cost-effective and large-area roll-to-roll fabrication, solution-processable OLEDs with higher efficiencies are extremely demanded.¹⁵⁻¹⁹

Over the past years, compared with vapor-deposited counterparts,²⁰⁻²³ wet-process feasible molecular hosts for phosphorescent OLEDs have rarely been reported.²⁴⁻³³ Kakimoto's group reported a maximum efficacy of 4.4 lmW⁻¹ by doping an Ir(ppy)₃ guest into triphenylamine/benzimidazole hybrid as host, *tris*(2-methyl-3'-(1-phenyl-1*H*-benzimidazol-2-yl)biphenyl-4-yl)amine.³² A maximum efficacy of 7.3 lmW⁻¹ was realized by doping a bipolar host, *tris*(2,2'-dimethyl-4'-(1-phenyl-1*H*-benzimidazol-2-yl)biphenyl-4-yl)amine with Ir(ppy)₃ guest.³³ Kido's group reported, at 100 cdm⁻², an efficacy of 11 lmW⁻¹ by employing a carbazole-type host, 1,3-bis(3-(3,6-di-*n*-butylcarbazol-9-yl)phenyl)benzene, and *tris*(2-(4-tolyl)phenylpyridine)iridium (III) as guest.³⁴ Jou and Grigalevicius's groups reported bipolar carbazole/phenylindole hybrid as host, 9,9'-bis[6-(carbazol-9-yl)hexyl][3,3']bicarbazole, and an efficacy of 16.4 lmW⁻¹ was realized by using Ir(ppy)₃ as guest.³⁵ Ma and Yang's groups achieved an efficacy of 26 lmW⁻¹ by using a oxadiazole/triphenylamine hybrid, 2-(3,5-bis(4'-(diphenylamino)phenyl)phenyl)-5-(4-*tert*-butylphenyl)-1,3,4-oxadiazole, as host.³⁶ Hence, synthesizing a wet-process feasible molecular host is greatly considerable in order to realize low cost, large-area, high throughput and high performance OLED based products.

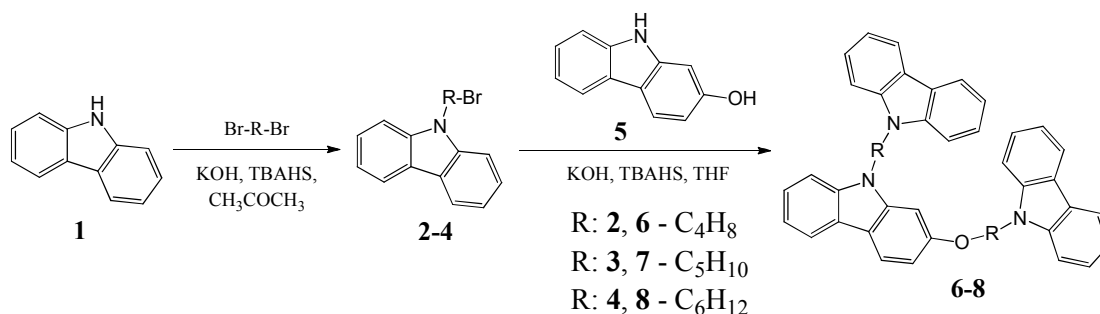
In this study, a high-efficiency, green phosphorescent OLED is presented by employing a wet-process feasible newly synthesized carbazole-type host material, 2-[4-(carbazol-9-yl)butyloxy]-9-[4-(carbazol-9-yl)butyl]carbazole (**6**) that possesses high triplet-energy and low carrier injection barrier. In the device doped with Ir(ppy)₃ guest, the host **6** exhibits a power efficiency of 51 lmW⁻¹ and current efficiency of 52 cdA⁻² at 100 cdm⁻². For comparison, two other hosts, 2-[5-(carbazol-9-yl)pentyloxy]-9-[5-(carbazol-9-yl)pentyl]carbazole (**7**) and 2-[6-(carbazol-9-yl)hexyloxy]-9-[6-(carbazol-9-

yl)hexyl]carbazole (**8**), were also studied. For host **7** containing device, its power efficiency was 29.1 lmW^{-1} (37.5 cdA^{-1}), while 23.3 lmW^{-1} (35.9 cdA^{-1}) for the compound **8**-containing counterpart.

3. Result and discussion

3.1 Synthesis of the host materials

Carbazole-type host materials, 2-[4-(carbazol-9-yl)butyloxy]-9-[4-(carbazol-9-yl)butyl]carbazole (**6**), 2-[5-(carbazol-9-yl)pentyloxy]-9-[5-(carbazol-9-yl)pentyl]carbazole (**7**) and 2-[6-(carbazol-9-yl)hexyloxy]-9-[6-(carbazol-9-yl)hexyl]carbazole (**8**), were synthesized using rather simple alkylation methods as shown in Scheme 1. The key starting materials, 9-(bromoalkyl)carbazoles (**2-4**) were prepared from commercially available 9*H*-carbazole (**1**) and an excess of corresponding dibromoalkane under basic conditions using tetra-*n*-butyl ammonium hydrogen sulphate (TBAHS) as phase transfer catalyst. The compounds **2-4** were reacted with 2-hydroxycarbazole (**5**) under basic conditions to afford the carbazolyl containing derivatives **6-8** as host materials. The newly synthesized derivatives were confirmed by ^1H NMR spectroscopy and mass spectrometry (*ESI* Figure S1, Figure S2 and Figure S3). The data were found to be in good agreement with the proposed structures. The derivatives were soluble in common organic solvents, such as acetone, chloroform or THF at room temperature.



Scheme 1. Schematic illustration of the synthesis of the carbazole-type hosts, **6**, **7**, and **8**.

3.2 Photophysical and electrochemical characteristics

Table 1 shows the photophysical properties of the three carbazole based host materials. **Figure 1** shows the ultraviolet-visible (UV-vis) and photoluminescence (PL) spectra of the materials **6-8** dissolved in tetrahydrofuran (THF) at room temperature. The singlet energy gaps were calculated from the inter-section of UV-vis absorption peaks, giving values of 3.54, 3.54 and 3.52 eV for compounds **6**, **7** and **8**, respectively.

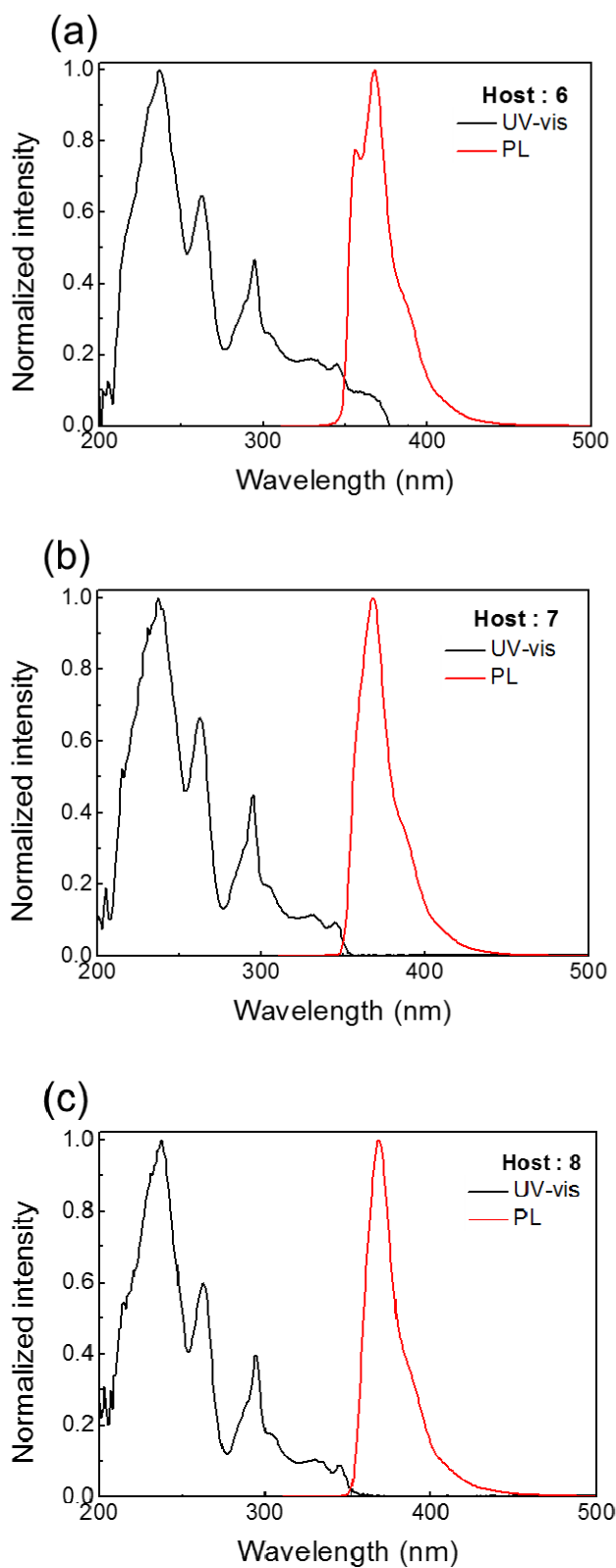


Figure 1. The ultraviolet-visible and photoluminescence spectra of the novel carbazole-type host materials, (a) **6**, (b) **7**, and (c) **8**. All the data were measured in tetrahydrofuran at room temperature.

The experimentally determined triplet-energies were 2.95 eV, 2.95 eV, and 2.96 eV for the materials **6**, **7** and **8**, respectively, which were calculated from the first phosphorescent emission peak of low temperature (77 K) PL spectra at 420 nm, 420 nm and 419 nm, as shown in **Figure 2(a)**. These results show Most importantly, the triplet-energies of these three host materials are extensively higher than that of the green emitter, Ir(ppy)₃, which exhibited a triplet-energy value of the 2.57 eV.^{37,38} These host materials should enable the occurrence of effective energy transfer from host-to-guest and exciton confinement on guest, resulting in good device efficiency.³⁹⁻⁴² Hence, these values of triplet energies are sufficiently higher to effectively confine the triplet excitons on the guest and extensively prohibit back energy transfer to the hosts. Both photophysical and electrochemical properties of all three hosts remain almost unchanged by increasing the length of alkyl and alkyl ether linkages.

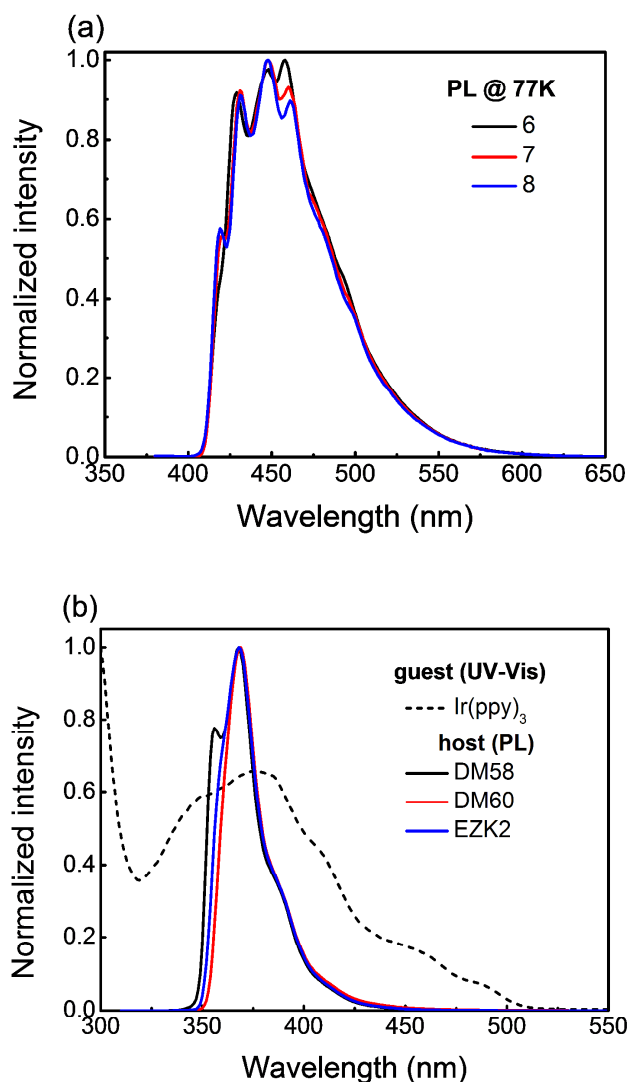


Figure 2. Photoluminescence (PL) spectra of the newly synthesized hosts **6**, **7**, and **8** measured in tetrahydrofuran (a) at 77 K and (b) at room temperature. Also shown is the ultraviolet-visible (UV-vis) spectrum of the green Ir(ppy)₃ guest molecule. The comparatively large overlapping area between the **6** host PL and the green emitter UV-vis spectra indicates a higher efficient host to guest energy transfer occurring in the **6**-containing green OLED.

The electrochemical properties of the three carbazole-type host molecules **6-8** are measured by cyclic voltammetry (*ESI Figure S4*). The highest occupied molecular orbital (HOMO) energy levels were estimated to be 5.48 eV, 5.48 eV, and 5.47 eV for **6**, **7**, and **8**, respectively, using oxidation potential. The lowest unoccupied molecular orbital (LUMO) energy levels of the emitters were calculated to be 1.95 eV, 1.95 eV, and 1.96 eV for **6**, **7**, and **8**, respectively, from HOMO energy levels and optical energy band gaps which estimated from the intersection of absorption and emission spectra (**Table 1**).

Table 1. Photophysical and electrochemical characteristics of the novel host **6**, comparing with those of the small molecular hosts **7** and **8**.

Host	λ_{ab} [nm]	λ_{em} [nm]	^{a)} E_T [eV]	^{b)} E_S [eV]	^{c)} HOMO [eV]	^{d)} LUMO [eV]	^{e)} T_g [°C]	^{f)} T_d [°C]
6	345	356, 368	2.95	3.54	5.48	1.95	64	361
7	345	368	2.95	3.54	5.48	1.95	58	345
8	345	369	2.96	3.52	5.47	1.96	20	338

^{a)}Triplet-energy level at 77K; ^{b)}Singlet energy-gap; ^{c)}HOMO values are measured by the cyclic voltammetry (CV) method. The semi-oxidation potential ($E_{1/2}^{ox}$) could be calculated from $(E_{p1}+E_{p2})/2-0.48$. Where 0.48 is correction value obtained by the oxidation system was added Ferrocenium/Ferrocene (Fc^+/Fc) as the internal standard, and then the energy of HOMO could be obtained from the $E_{HOMO} = -(E_{1/2}^{ox} + 4.8)$. ^{d)}The energy of LUMO could be obtained by subtracting the optical bandgap from the HOMO energy level, [$E_{LUMO} = (E_{HOMO} - E_g)$]; ^{e)} Glass transition temperature; ^{f)}Thermal decomposition temperature.

3.3 Thermal characteristics

As measured using differential scanning calorimetry (DSC), the host molecule **6** shows a glass transition temperature (T_g) of 64 °C, while 58 °C for **7** and 20 °C for **8** (**Table 1**). The slightly higher T_g of the host **6** indicated a strong intermolecular interaction of carbazole units owing to short chain alkyl ether and alkyl junctions. As investigated using thermogravimetric analysis (TGA), the host **6** exhibits a thermal decomposition temperature (T_d) of 361 °C, corresponding to a 5 % weight loss, while 345 °C for **7** and 338 °C for **8**. The higher T_g and T_d characteristic of the host **6** facilitates relatively better film integrity during the entire fabrication process, especially during solvent removal.^{43,44}

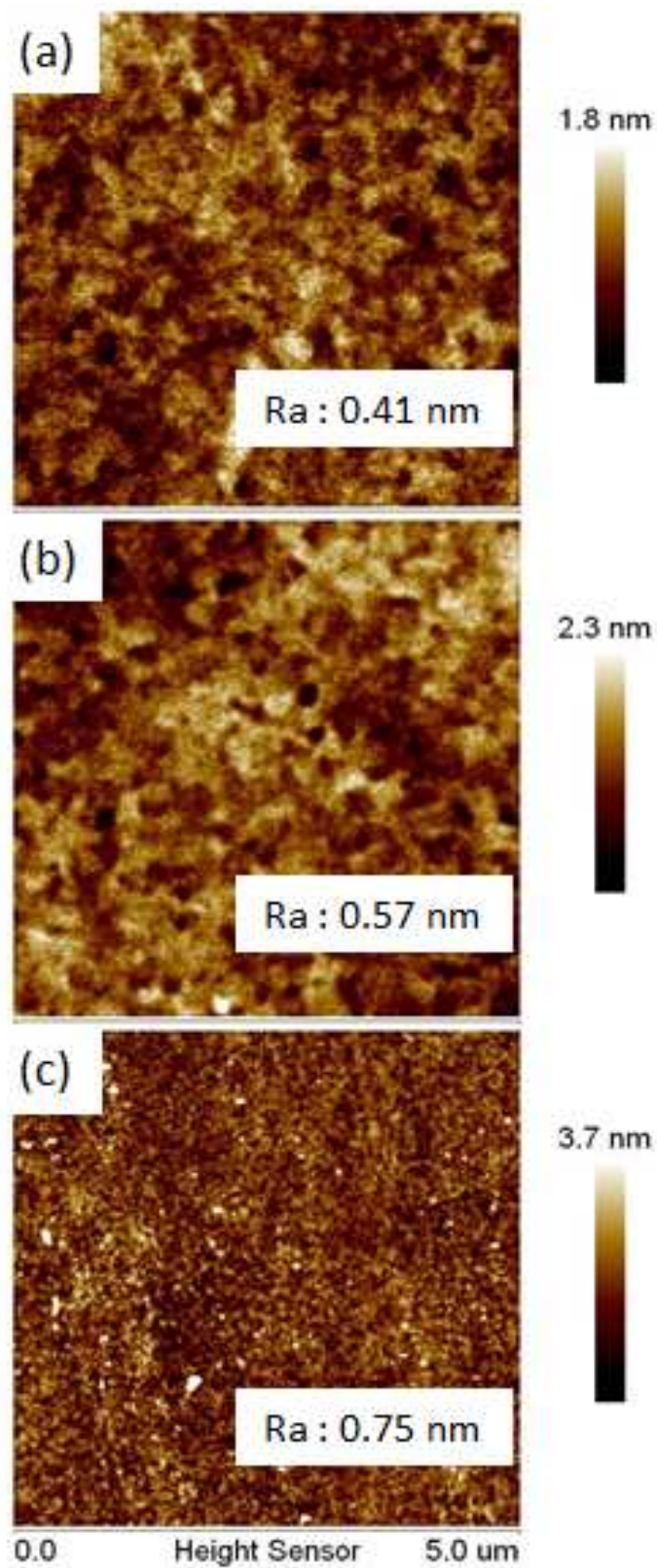


Figure 3. Surface morphologies of the spin-coated films that comprise the pure hosts (a) **6**, (b) **7**, and (c) **8**. All the films uniformities are improved upon increasing the glass transition temperature (T_g).

Figure 3 shows the atomic-force microscope (AFM) images of the compounds, **6**, **7**, and **8** containing films by spin-coating. The respective surface roughness values are 0.41, 0.57 and 0.75 nm, while the corresponding glass transition temperatures (T_g) are 65, 58 and 20 °C. The surface roughness becomes smoother as the T_g of the host material is increased. The somewhat better film integrity may explain why compound **7** containing device shows better device efficiency than the compound **8** containing counterpart.

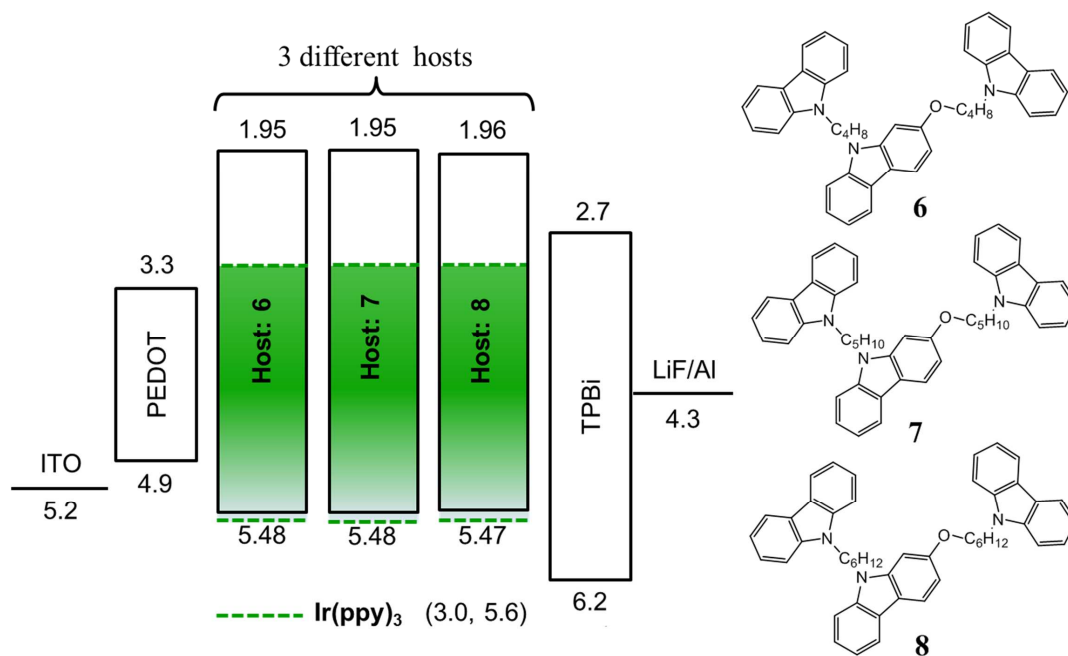


Figure 4. Schematic diagram of the energy-levels of the OLED device containing the presented host materials, **6**, **7**, and **8**. Also shown the molecular structures of the three studied hosts.

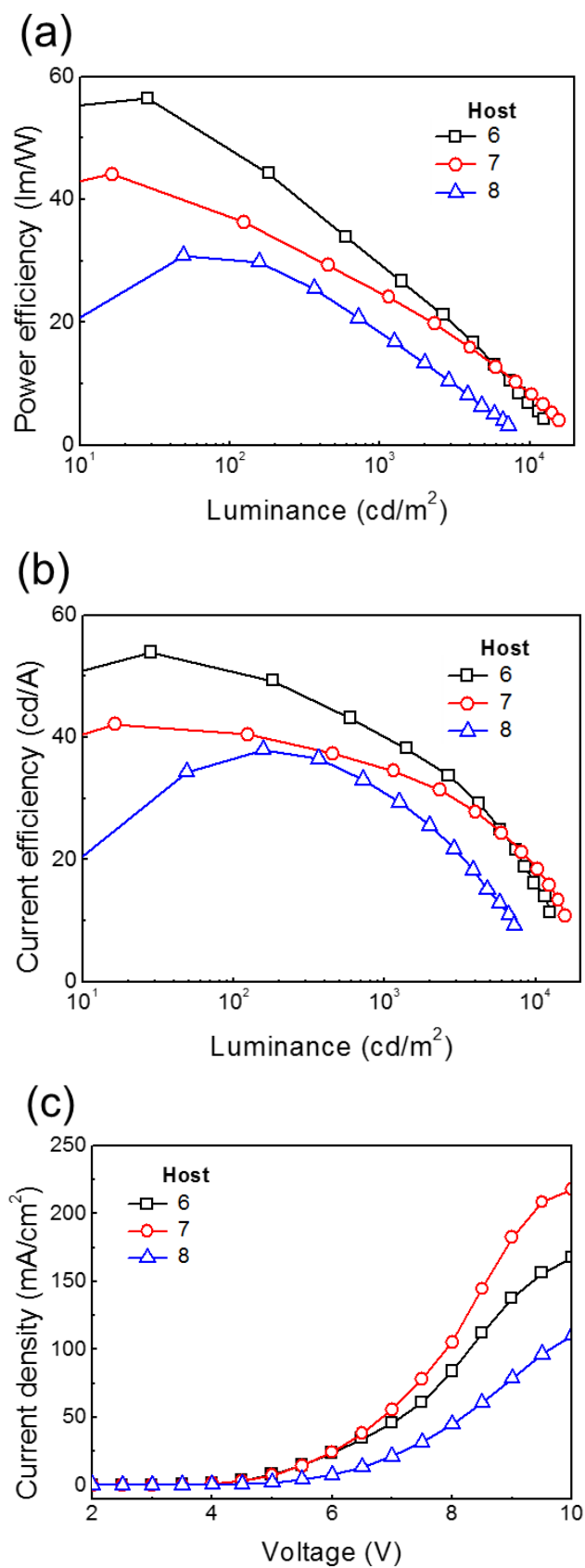
3.4 Electroluminescent characteristics of devices

Figure 4 illustrates the schematic energy-level diagram of green OLED devices and the molecular structures of newly synthesized host materials, **6**, **7**, and **8**. The devices are composed of a 125 nm indium tin oxide (ITO) anode layer, a 35 nm poly(3,4-ethylene-dioxythiophene)-poly(styrenesulfonate) (PEDOT:PSS) hole injection layer (HIL), a 20 nm single emissive layer (EML) with the Ir(ppy)₃ emitter doped in compound **6** host via spin-coating, a 32 nm 1,3,5-tris(*N*-phenyl-benzimidazol-2-yl)benzene (TPBi) electron transporting layer (ETL), a 1 nm lithium fluoride (LiF) layer, and a 100 nm aluminum (Al) cathode layer. Besides the host **6**, two other compounds, **7** and **8**, were also studied for comparison.

Table 2. Effects of the different doping concentrations of Ir(ppy)₃ on the operation voltage (OV), power efficiency (η_p), current efficiency (η_c), external quantum efficiency (η_{ext}) and CIE coordinates of the novel host materials **6**, **7**, and **8**-containing OLED devices.

Host	Wt% ratio of dopant	OV [V]	η_p [lm/W]	η_c [cd/A]	η_{ext} [%]	1931 CIE Coordinates	Maximum luminance [cd/m ²]
6	5	4.7/ 6.0	22.7/ 14.1	34.0/ 26.7	9.5/ 7.4	(0.29, 0.63)/ (0.29, 0.63)	7899
	10	4.0/ 5.2	33.8/ 21.5	43.3/ 35.2	11.6/ 9.5	(0.30, 0.63)/ (0.30, 0.63)	11010
	15	3.6/ 4.7	36.3/ 23.2	41.8/ 34.5	11.5/ 9.5	(0.32, 0.62)/ (0.32, 0.62)	13800
	16.7	3.5/ 4.5	44.6/ 26.9	49.8/ 38.7	13.6/ 10.6	(0.31, 0.63)/ (0.31, 0.63)	11250
	20	3.2/ 4.3	50.8/ 30.3	51.8/ 40.7	14.1/ 11.1	(0.31, 0.63)/ (0.31, 0.63)	12600
	23	3.0/ 3.9	37.9/ 28.3	36.7/ 34.5	10.1/ 9.5	(0.33, 0.62)/ (0.32, 0.62)	14510
	7	5	6.9/ 8.5	25.4/ 14.3	55.6/ 38.8	7.5/ 6.0	(0.30, 0.63)/ (0.30, 0.63)
10		6.4/ 8.1	27.7/ 16.2	56.3/ 41.8	7.8/ 6.5	(0.31, 0.63)/ (0.31, 0.63)	8447
15		4.0/ 5.5	32.1/ 18.5	40.8/ 32.4	10.6/ 7.3	(0.32, 0.62)/ (0.32, 0.62)	8954
20		3.7/ 4.9	39.5/ 24.2	46.7/ 38.1	12.0/ 9.2	(0.32, 0.62)/ (0.32, 0.62)	12750
25		3.4/ 4.4	38.0/ 25.2	40.8/ 35.1	12.2/ 9.6	(0.33, 0.62)/ (0.33, 0.62)	15730
30		3.1/ 4.1	42.5/ 29.1	42.2/ 37.5	9.9/ 8.6	(0.33, 0.62)/ (0.33, 0.62)	17810
8		5	3.5/ 4.6	25.2/ 15.9	28.4/ 23.1	15.1/ 10.3	(0.30, 0.63)/ (0.30, 0.63)
	10	4.6/ 6.0	22.3/ 13.0	32.4/ 25.1	14.8/ 11.3	(0.30, 0.63)/ (0.30, 0.63)	7767
	15	4.3/ 5.6	31.1/ 16.2	41.9/ 28.8	10.6/ 8.9	(0.30, 0.63)/ (0.30, 0.63)	9028
	20	3.8/ 4.9	38.1/ 23.3	46.0/ 35.9	13/ 10.4	(0.31, 0.63)/ (0.31, 0.63)	10830
	30	3.5/ 5.1	39.0/ 21.4	43.9/ 34.6	11.3/ 9.8	(0.33, 0.62)/ (0.32, 0.62)	9252
	35	3.7/ 5.3	30.4/ 18.7	36.1/ 31.1	10.6/ 10.1	(0.32, 0.62)/ (0.32, 0.62)	7194

Table 2 shows the electroluminescent characteristics of the host **6** containing green OLED, comparing with that of the **7** and **8**-containing counterparts. As shown in **Figure 5**, host **6** containing device exhibited the power efficiency of 30.3 lmW⁻¹ with current efficiency of 40.7 cdA⁻¹ at 1,000 cdm⁻², highest among all three host containing devices. For host **7** containing device, its power efficiency was 29.1 lmW⁻¹ (37.5 cdA⁻¹), while 23.3 lmW⁻¹ (35.9 cdA⁻¹) for the host **8** containing counterpart.



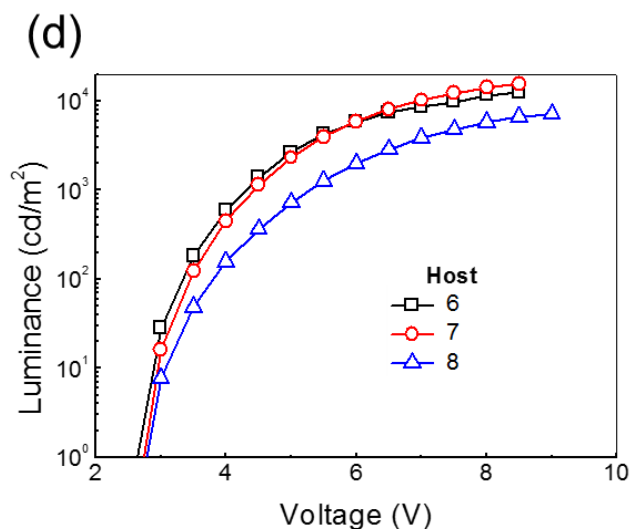
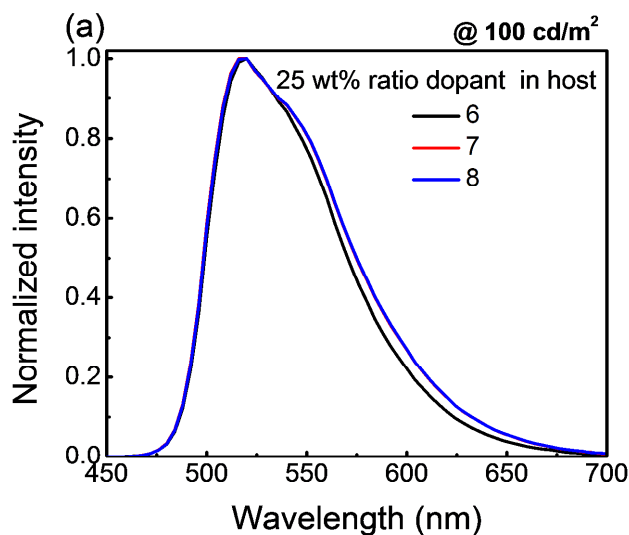


Figure 5. Compares the (a) power efficiency, (b) current efficiency, (c) current density, and (d) luminance of the devices with the 25 wt% ratio $\text{Ir}(\text{ppy})_3$ doped in the host materials, **6**, **7** and **8**, studied herein.

As illustrated in **Figure 4**, the architectures of the three hosts, **6**, **7**, and **8**, containing device much favors the injection of holes to the hosts because they exhibit a hole injection barrier of around 0.58 eV, which is 0.12 eV lower than that of the hole to the guest (0.7 eV). Whilst, the same architectures favor the injection of electron into the $\text{Ir}(\text{ppy})_3$ guest because there exist a -0.2 eV electron trap, while there is an around 0.75 eV barrier for electron to enter into the hosts. These would hence lead excitons to generate on both host and guest and result in a high device efficiency [19].



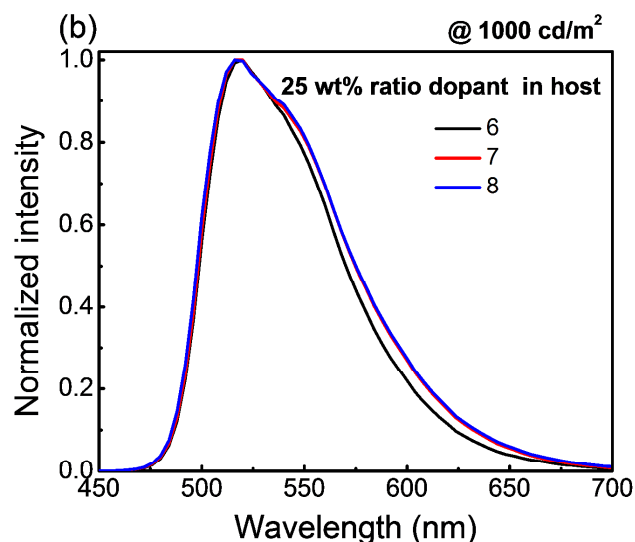
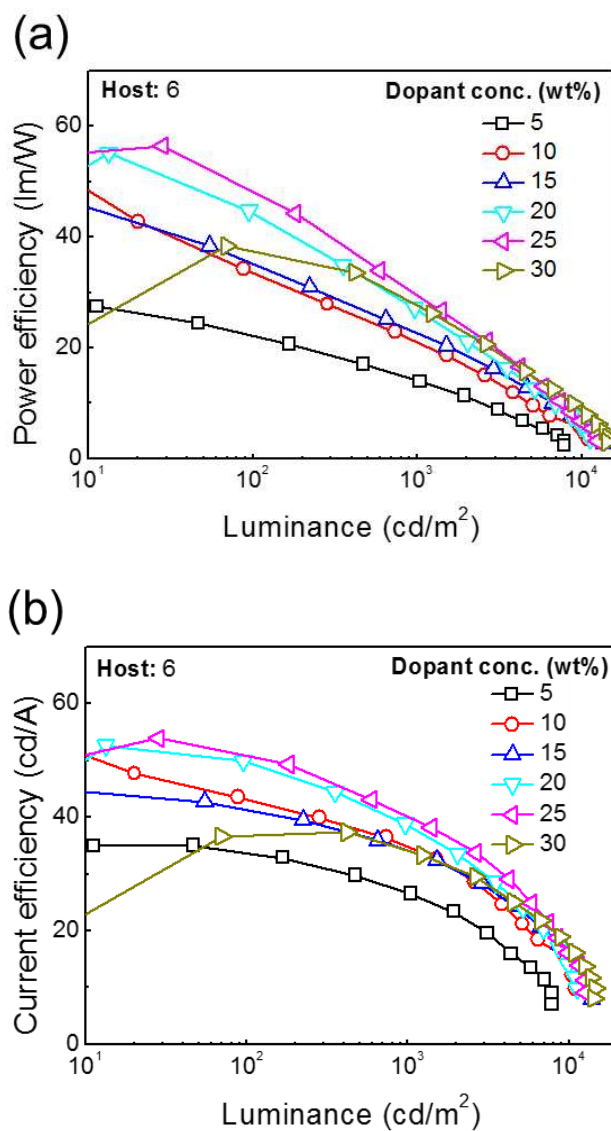


Figure 6. Host effect on the electroluminescence (EL) spectra of the devices containing the three different host molecules, **6**, **7** and **8**, with 25 wt% ratio green emitter, Ir(ppy)₃. The EL emission spectrum becomes slightly broader as the host material is changed from **6** to **7** or **8**, while the spectra remain unchanged even at higher luminance, 1000 cdm⁻².

Amongst, compound **6** containing device showed a highest efficiency. The reason why the EL properties, including power efficiency, current efficiency and EQE, were different for the devices containing the three compounds **6**, **7** and **8** may be attributed to the difference in effectiveness of host-to-guest energy transfer. As shown in **Figure 2 (b)**, the overlapping area between the absorption spectrum of guest (UV-vis of Ir(ppy)₃) and the emission spectrum of host (PL) was the largest for compound **6**, indicating a comparatively highest host-to-guest energy transfer. Furthermore, compound **6** showed an additional emission peaking at the lower wavelength site (356 nm), which would hence trigger the higher energy emission of the guest. This explains why the resultant electroluminescent (EL) spectrum of the green Ir(ppy)₃ doped into compound **6** was blue-shifted as comparing with those into compounds **7** and **8** as host, as shown in **Figure 6**. There is only guest, Ir(ppy)₃, emission without any emission from hosts. This shows that the energy was much effectively transferred from the host to the guest.

As shown in **Figure 7**, the device efficiency is extensively depended on doping concentration of the green emitter. Taking the host **6**-based device for example, the power efficiency at 1,000 cdm⁻² is increased from 14.1 to 30.3 lmW⁻¹ as doping concentration is increased from 5 to 25 wt%. The resulting device shows the highest efficiency among all studied concentrations, as 25 wt% guest was doped into the host **6**. However, as the concentration is increased to 30 wt%, the power efficiency starts to drop. This may be

attributed to the concentration-quenching efficiency roll-off, resulting from self-segregation of the emitter at high concentrations.



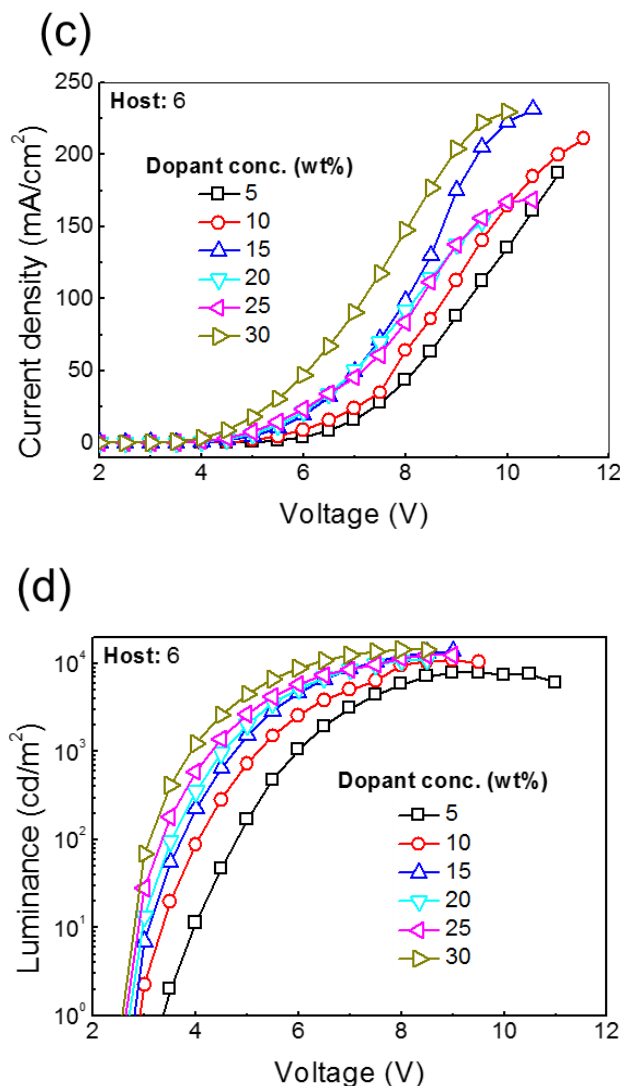


Figure 7. Doping concentration (weight ratio with host) effects on the (a) power efficiency, (b) current efficiency, (c) current density, and (d) luminance results of the **6** host based green OLED device.

When material **8** was employed as the host, the resultant device exhibits the power efficiency of 15.9 lmW⁻¹ (23.1 cdA⁻¹), at 1,000 cdm⁻², with a 5 wt% doping concentration of Ir(ppy)₃ guest. The efficiency becomes higher as the dopant concentration increases from 5 to 20 wt%. At 20 wt%, for example, the power efficiency is 23.3 lmW⁻¹ (35.9 cdA⁻¹). As dopant concentration further increases to 35 wt%, the efficacy drops to 18.7 lmW⁻¹ (31.1 cdA⁻¹). For host **7** containing device showed the best efficacy of 29.1 lmW⁻¹ (35.9 cdA⁻¹) with a 30 wt% doping concentration of Ir(ppy)₃. Compared to that of the counterpart **8**, the higher efficiency exhibited by the host **7** containing device may result mainly from the fact that the material **8** shows the poor film integrity owing to relatively much lower T_g of 20 °C.

Furthermore, we have investigated the effect of all the three hosts, **6**, **7** and **8** devices operational stability, t_{50} , based on solution-process feasible emissive layer. The operational lifetime of all devices were investigated without encapsulation. As measured at an initial brightness of 800 cdm^{-2} , the resultant operational lifetime values have shown the operational stability of 27, 12 and 5.4 min., respectively, for compounds **6**, **7** and **8** (*ESI Figure 5*).

4. Conclusion

To conclude, we demonstrate in this report a molecular carbazole-based host **6**, with wet-process feasibility. By employing this host, green phosphorescent OLED devices with higher efficiencies have been fabricated. The resulting device shows, at 100 cdm^{-2} for example, a power efficiency of 51 lmW^{-1} and current efficiency of 52 cdA^{-1} for a simple double layer green phosphorescent OLED device. The high efficiency may be attributed to the host possessing an effective host-to-guest energy transfer. The facile synthesis, excellent solubility in common organic solvents, excellent film integrity and very high triplet energy come together to ensure that the compound **6** may be a promising host material for low cost and large-area roll-to-roll fabrication of energy-efficient phosphorescent OLEDs.

5. Experimental methods

5.1 Materials characteristics and measurements: All the precursor compounds required for the synthesis were purchased from commercial sources and used as such without further purification. Column chromatography purifications were performed with silica gel (70-230 mesh) as a stationary phase in a column with 50 cm long and 5 cm diameter. ^1H NMR spectra were recorded using a Varian Unity Inova (300 MHz) apparatus. Mass spectra of the compounds were obtained on a Waters ZQ 2000 spectrometer in the positive ion mode. The EL spectra were recorded in tetrahydrofuran at room temperature in quartz cuvettes using a Fluorolog III photoluminescence spectrometer. UV-vis spectra were recorded in toluene at room temperature using a UV-Vis spectrophotometer.

Cyclic voltammetry (CV) experiments were performed on an electrochemical workstation using a three electrode assembly comprising glassy carbon working electrode, a non-aqueous Ag/AgCl reference electrode and an auxiliary platinum electrode. The experiments were performed at room temperature under nitrogen atmosphere in dichloromethane using 0.1 M tetrabutylammonium perchlorate (Bu_4NClO_4) as supporting electrolyte on a Chinstruments CH1604A potentiostat. The $E_{1/2}^{\text{ox}}$ values were determined as $(E_p^{\text{a}} + E_p^{\text{c}})/2$, where E_p^{a} and E_p^{c} are the anodic and cathodic peak potentials, respectively.

Differential scanning calorimetry (DSC) measurements were carried out using a Bruker Reflex II thermosystem. The DSC curves were recorded in a nitrogen atmosphere at a heating rate of 10 °C/min. Thermogravimetric analysis (TGA) and was performed under a continuous nitrogen flow using a TGA Q50 apparatus at heating rate of 10 °C/min.

5.2 Device fabrication and characterization: **Figure 4** shows the schematic energy-level diagram of green OLEDs studied herein. The fabrication process included firstly spin-coating an aqueous solution of PEDOT:PSS at 4,000 rpm for 20 s to form a hole-injection layer (HIL) on a pre-cleaned ITO anode. Before depositing the following emissive layer, the solution was prepared by dissolving the Ir(ppy)₃ guest in three different novel host molecules, **6**, **7** and **8**, in tetrahydrofuran at room-temperature for 0.5 h with stirring. The resulting solution was then spin-coated at 2,500 rpm for 20 s under nitrogen. Followed were the depositions of the electron-transporting layer TPBi, the electron injection layer LiF, and the cathode Al, by thermal evaporation in a vacuum chamber at the vacuum level of less than 5×10^{-6} Torr.

The luminance, CIE chromatic coordinates, and electroluminescent spectrum of the resultant yellow OLEDs were measured by using Photo Research PR-655 spectrascan. Keithley 2400 electrometer was used to measure the current-voltage (I–V) characteristics. The emission area of the devices was 25 mm², and only the luminance in the forward direction was measured.

Acknowledgement

This work was financially supported by National Science Council through the grant numbers of 100-2119-M-007-011-MY3 and 103-2923-E-007-003-MY3, Ministry of Economic Affairs through the grant number MEA 102-EC-17-A-07-S1-181 and by Research Council of Lithuania (project TAPLLT1/14).

References

1. F. So, J. Kido and P. Burrows, *MRS Bull.*, 2008, **33**, 663.
2. B. W. D'Andrade and S. R. Forrest, *Adv. Mater.*, 2004, **16**, 1585.
3. M. C. Gather, A. Kohnen and K. Meerholz, *Adv. Mater.*, 2011, **23**, 233.
4. S. R. Forrest, *Nature*, 2004, 428, 911.
5. S. Reineke, F. Lindner, G. Schwartz, N. Seidler, K. Walzer, B. Lussem and K. Leo, *Nature*, 2009, **459**, 234.

6. M. A. Baldo, D. F. O'Brien, Y. You, A. Shoustikov, S. Sibley, M. E. Thompson and S. R. Forrest, *Nature*, 1998, **395**, 151.
7. C. Adachi, M. A. Baldo and S. R. Forrest, *Appl. Phys. Lett.*, 2000, **77**, 904.
8. J. P. Duan, P. P. Sun and C. H. Cheng, *Adv. Mater.*, 2003, **15**, 224.
9. Q. Zhang, Q. Zhou, Y. Cheng, L. Wang, D. Ma and X. Jing, *Adv. Mater.*, 2004, **16**, 432.
10. S.-J. Yeh, M.-F. Wu, C.-T. Chen, Y.-H. Song, Y. Chi, M.-H. Ho, S.-F. Hsu and C.-H. Chen, *Adv. Mater.*, 2005, **17**, 285.
11. R. J. Holmes, S. R. Forrest, Y.-J. Tung, R. C. Kwong, J. J. Brown, S. Garon and M. E. Thompson, *Appl. Phys. Lett.*, 2003, **82**, 2422.
12. S. Tokito, T. Iijima, Y. Suzuri, H. Kita, T. Tsuzuki and F. Sato, *Appl. Phys. Lett.*, 2003, **83**, 569.
13. S.-J. Su, H. Sasabe, T. Takeda and J. Kido, *Chem. Mater.*, 2008, **20**, 1691.
14. S.-J. Su, C. Cai and J. Kido, *Chem. Mater.*, 2011, **23**, 274.
15. J. S. Chen, C. S. Shi, Q. Fu, F. C. Zhao, Y. Hu, Y. L. Feng, and D. G. Ma, *J. Mater. Chem.*, 2012, **22**, 5164.
16. T.-W. Lee, T. Noh, H.-W. Shin, O. Kwon, J.-J. Park, B.-K. Choi, M.-S. Kim, D. W. Shin, and Y.-R. Kim, *Adv. Mater.*, 2009, **19**, 1625.
17. J.-H. Jou, M.-F. Hsu, W.-B. Wang, C.-L. Chin, Y.-C. Chung, C.-T. Chen, J.-J. Shyue, S.-M. Shen, M.-H. Wu, W.-C. Chang, C.-P. Liu, S.-Z. Chen and H.-Y. Chen, *Chem. Mater.*, 2009, **21**, 2565.
18. J.-H. Jou, C.-J. Li, S.-M. Shen, S.-H. Peng, Y.-L. Chen, Y.-C. Jou, J. H. Hong, C.-L. Chin, J.-J. Shyue, S.-P. Chen, J.-Y. Li, P.-H. Wang and C.-C. Chen, *J. Mater. Chem. C*, 2013, **1**, 4201.
19. J.-H. Jou, Y.-M. Yang, S.-Z. Chen, J.-R. Tseng, S.-H. Peng, C.-Y. Hsieh, Y.-X. Lin, C.-L. Chin, J.-J. Shyue, S.-S. Sun, C.-T. Chen, C.-W. Wang, C.-C. Chen, S.-H. Lai and F.-C. Tung, *Adv. Optical Mater.*, 2013, **1**, 657.
20. F.-M. Hsu, C.-H. Chien, P.-I. Shih and C.-F. Shu, *Chem. Mater.*, 2009, **21**, 1017.
21. Z.-Q. Gao, M. Luo, X.-H. Sun, H.-L. Tam, M.-S. Wong, B.-X. Mi, P.-F. Xia, K.-W. Cheah, and C.-H. Chen, *Adv. Mater.*, 2009, **21**, 688.
22. T. Zhang, Y. Liang, J. Cheng, J. Li, *J. Mater. Chem. C*, 2013, **1**, 757.
23. H. Sasabe, T. Chiba, S.-J. Su, Y.-J. Pu, K. Nakayama, J. Kido, *Chem. Commun.* 2008, 5821.
24. L. Duan, L. Hou, T.-W. Lee, Juan Qiao, D. Zhang, G. Dong, L. Wang and Y. Qiu, *J. Mater. Chem.*, 2010, **20**, 6392.

25. L. Zeng, T. Y.-H. Lee, P. B. Merkel and S. H. Chen, *J. Mater. Chem.*, 2009, **19**, 8772.
26. D'Andrade, B. W.; Baldo, M. A.; Adachi, C.; Brooks, J.; Thompson, M. E.; Forrest and S. R. *Appl. Phys. Lett.*, 2001, **79**, 1045.
27. C. Adachi, M. A. Baldo, M. E. Thompson and S. R. Forrest, *J. Appl. Phys.*, 2001, **90**, 5048.
28. M. Ikaia, S. Tokito, Y. Sakamoto, T. Suzuki, and Y. Taga, *Appl. Phys. Lett.*, 2001, **79**, 156.
29. Y. Qian, F. Cao and W. Guo, *Tetrahedron*, 2013, **69**, 4169.
30. P. I. Shih, C. L. Chiang, A. K. Dixit, C. K. Chen, M. C. Yuan, R. Y. Lee, C. T. Chen, E. W. G. Diau and C. F. Shu, *Org. Lett.*, 2006, **8**, 2799.
31. S. Tokito, T. Lijima, Y. Suzuri, H. Kita, T. Tsuzuki and F. Sato, *Appl. Phys. Lett.*, 2003, **83**, 569.
32. Z. Ge, T. Hayakawa, S. Ando, M. Ueda, T. Akiike, H. Miyamoto, T. Kajita, M. Kakimoto, *Chem. Mater.*, 2008, **20**, 2532.
33. Z. Ge, T. Hayakawa, S. Ando, M. Ueda, T. Akiike, H. Miyamoto, T. Kajita, M. Kakimoto, *Adv. Funct. Mater.*, 2008, **18**, 584.
34. N. Aizawa, Y.-J. Pu, H. Sasabe, J. Kido, *Org. Electron.*, 2012, **13**, 2235.
35. D. Mazetyte, G. Krucaite, J. Grazulevicius, C.-I. Chiang, F.-C. Yang, J.-H. Jou, S. Grigalevicius, *Opt. Mater.*, 2013, **35**, 604.
36. M. Zhu, T. Ye, X. He, X. Cao, C. Zhong, D. Ma, J. Qin, C. Yang, *J. Mater. Chem.*, 2011, **21**, 9326.
37. N. Li, S.-L. Lai, W. Liu, P. Wang, J. You, C.-S. Lee, and Z. Liu, *J. Mater. Chem.*, 2011, **21**, 12977.
38. X. Yang, D. Neher, D. Hertel, and T. K. Däubler, *Adv. Mater.*, 2004, **16**, 161-166.
39. S. Tokito, T. Iijima, Y. Suzuri, H. Kita, T. Tsuzuki and F. Sato, *Appl. Phys. Lett.*, 2003, **83**, 569.
40. A. P. Kulkarni, C. J. Tonzola, A. Babel and S. A. Jenekhe, *Chem. Mater.*, 2004, **16**, 4556; G. Hughes and M. R. Bryce, *J. Mater. Chem.*, 2005, **15**, 94.
41. Y. Kawamura, S. Yanagida and S. R. Forrest, *J. Appl. Phys.*, 2002, **92**, 87.
42. P. A. Vecchi, A. B. Padmaperuma, H. Qiao, L. S. Sapochak and P. E. Burrows, *Org. Lett.*, 2006, **8**, 4211.
43. J.-H. Jou, W.-B. Wang, S.-Z. Chen, J.-J. Shyue, M.-F. Hsu, C.-W. Lin, S.-M. Shen, C.-J. Wang, C.-P. Liu, C.-T. Chen, M.-F. Wu, and S.-W. Liu, *J. Mater. Chem.*, 2010, **20**, 8411.

44. J.-H. Jou, W.-B. Wang, S.-M. Shen, S. Kumar, I.-M. Lai, J.-J. Shyue, S. Lengvinaite, R. Zostautiene, J. V. Grazulevicius, S. Grigalevicius, S.-Z. Chen and C.-C. Wu, *J. Mater. Chem.*, 2011, **21**, 9546.

Graphical abstract

Wet-process feasible high triplet energy carbazole based host material are synthesized. Doping a green phosphorescent emitter *fac* tris(2-phenylpyridine)iridium ($\text{Ir}(\text{ppy})_3$) into host 2-[4-(carbazol-9-yl)butyloxy]-9-[4-(carbazol-9-yl)butyl]carbazole (**6**), the device shows an efficacy of 51 lmW^{-1} and current efficiency of 52 cdA^{-1} at 100 cdm^{-2} or 30 lmW^{-1} and 40.7 cdA^{-1} at $1,000 \text{ cdm}^{-2}$.

